Available online at www.sciencedirect.com

SCIENCE DIRECT®

Journal of Applied Geophysics 56 (2004) 17–29

JOURNAL OF APPLIED GEOPHYSICS

www.elsevier.com/locate/jappgeo

High-resolution electrical imaging of the Varco d'Izzo earthflow (southern Italy)

A. Perrone[a,*], A. Iannuzzi[a], V. Lapenna[a], P. Lorenzo[b], S. Piscitelli[a], E. Rizzo[a], F. Sdao[b]

[a] *Istituto di Metodologie per l'Analisi Ambientale, C.N.R., C.da S. Loja, 85050 Tito (PZ), Italy*

[b] *Dipartimento di Strutture, Geotecnica, Geologia Applicata all'Ingegneria, Università della Basilicata, Loc. Macchia Romana, 85100 Potenza, Italy*

Received 1 November 2002; accepted 15 March 2004

Abstract

Geoelectrical prospecting techniques have been applied in the study of the Varco d'Izzo landslide, one of the most interesting of its type. It is characterized by a rototranslational movement in the early stage and successively has undergone earthflow-type movement, which still continues today. This landslide is located in the Southern Apennine area near the city of Potenza (Italy). In particular, electrical resistivity tomographies (ERT) and self-potential surveys (SP) have been carried out by combining modern technologies for data acquisition and new methods for data inversion. The high resolution of the electrical tomographic images helped us to accurately describe the geometry of this landslide body. Joint interpretation of geophysical, geological and geomorphological data allowed us to identify the sliding surface, estimate the thickness of the mobilized material and describe the main patterns of the subsurface fluid flows in Varco d'Izzo landslide.

Keywords: Rototranslational-earthflow landslide; Southern Apennine chain; Geoelectrics; Resistivity; Self-potential; Tomography

1. Introduction

Many geophysical methodologies are often applied for studying and monitoring a wide class of hydrogeological phenomena. In particular, different geophysical techniques (seismics, geoelectrics, magnetometry, gravimetry, thermometry, GPS, etc.) produce significant results in the investigation of landslide areas. The main objectives of geophysical surveys are: (1) geometrical reconstruction of landslide bodies (lateral extension and thickness); (2) identification of sliding surfaces found between the landslide body and the underlying bedrock; and (3) studying the movements and accumulations of groundwater flows that may provoke landslide reactions (McCann and Forster, 1990; Bruno and Marillier, 2000; Gallipoli et al., 2000; Hack, 2000; Mauritsch et al., 2000; Lapenna et al., 2003). Recently, great attention has been focused on geoelectrical techniques, such as electrical resistivity tomography (ERT) (Griffiths and Barker, 1993; Loke and Barker, 1996; Giano et al., 2000; Schmutz et al., 2000) and self-potential (SP) techniques (Bogoslovsky and Ogilvy, 1977; Patella et al., 1995; Bruno et al., 1998; Revil et al., 2002). Both methods show high spatial resolution capability and

* Corresponding author.
E-mail address: perrone@imaa.cnr.it (A. Perrone).

0926-9851/$ - see front matter © 2004 Elsevier B.V. All rights reserved.
doi:10.1016/j.jappgeo.2004.03.004

are characterized by relatively fast field data acquisition and low costs. Furthermore, the development of innovative and robust inversion methods (Loke and Barker, 1996; Patella, 1997) provides a more accurate data interpretation that can be used for resolving complex geological problems, such as defining aspects of hidden underground structures (i.e. faults, underground water bodies, etc.) and studying the space-temporal evolution of groundwater flow movements related to landslide phenomena.

As a part of a project on geophysical monitoring of landslides in the Southern Apennine chain financed by the Italian Ministry of University and Research, we carried out a geoelectrical survey based on tomographic approaches with the purpose of acquiring a better knowledge about a landslide, having both rototranslational as well as earthflow characteristics, which involves the village of Varco d'Izzo, near the city of Potenza located in the Lucanian Apennine chain (Southern Italy) (Fig. 1).

The Basilicata Region is one of the most landslide affected areas in Southern Italy. This is principally because major part of the region is covered by clayey terrains and is affected by extreme rainfall events. In Basilicata, all forms of landslide can be found, but in particular, we encounter rotational and translational slides and earthflow.

About 48% of all Italian towns affected by hydrogeological instability phenomena are located in Southern Italy and 51% of the areas showing the highest level of landslide risk are also found there. An average area of 100 km^2 in Italy is affected by five landslides. In Basilicata, the same area is affected by 27 landslides (Gullà and Sdao, 2001), thus demonstrating that Basilicata is a natural laboratory for practical application and validation of new investigation techniques.

From a geological point of view, the investigated area is affected by still active rototranslational-earthflow phenomena, which involves complex clayey-marly terrains referred to as Argille Varicolori Formation (Upper Cretaceous–Lower Oligocene) (Bonardi et al., 1988). Furthermore, the landslide in Varco d'Izzo caused damages to residences, roads and, especially, to the main highway (SS 407 Basentana) and railway line (Potenza–Metaponto line). The latter is an important connection between the Tyrrhenian and the Ionian coast.

During our geoelectrical surveys, a dipole–dipole multielectrode array, connected to a 24-bit A/D acquisition unit, was used. Tomographic algorithms were applied for resistivity and self-potential data inversion (Loke and Barker, 1996; Patella, 1997), and high-resolution images of the subsurface electrical properties were obtained. The resistivity tomographies, integrated with data coming from direct soundings, allowed us to depict the geometry of the sliding surface and to estimate the thickness of the sliding material found in the accumulation zone. The SP map and tomography panels helped us to describe the main patterns of the subsurface fluid flows in the Varco d'Izzo earthflow.

2. Geological and geomorphological setting

The Varco d'Izzo landslide (Potenza, Southern Italy) is one of the most dangerous mass movements of the whole Lucanian Apennine Chain. It is an active rototranslational slide, i.e., a complex mass movement occurring dominantly on a partly planar and partly curved detachment, that evolved into an earthflow (Cruden and Varnes, 1996). The landslide is approximately 1400 m long, about 130–420 m wide and extends between 850 and 620 m a.s.l. (Basento River) and has a mean inclination of about 10° (Fig. 1).

In the area, structurally complex clayey-marly terrains referred to as Argille Varicolori (Upper Cretaceous–Lower Oligocene) outcrop. They are composed of intensively tectonized fissured and shared clay shales, clay and mudstones, green, red, black, yellow and grey in colour which locally include disarranged blocks and layers of lapideous rocks, such as marls, calcarenites or limestones.

Geological and geomorphologic in situ surveys, aerial photo analyses and data interpretation from previous direct soundings, which reached the bottom of the detachment zone (Curcetti, 1996; Polemio and Sdao, 1996), allowed us to approximately define the limits of the landslide body and to estimate the thickness of its displaced material for different sectors of the landslide.

In Fig. 2, the main geomorphologic features of the landslide, along with the location in which the geologic and geophysical surveys were carried out, have been summarised.

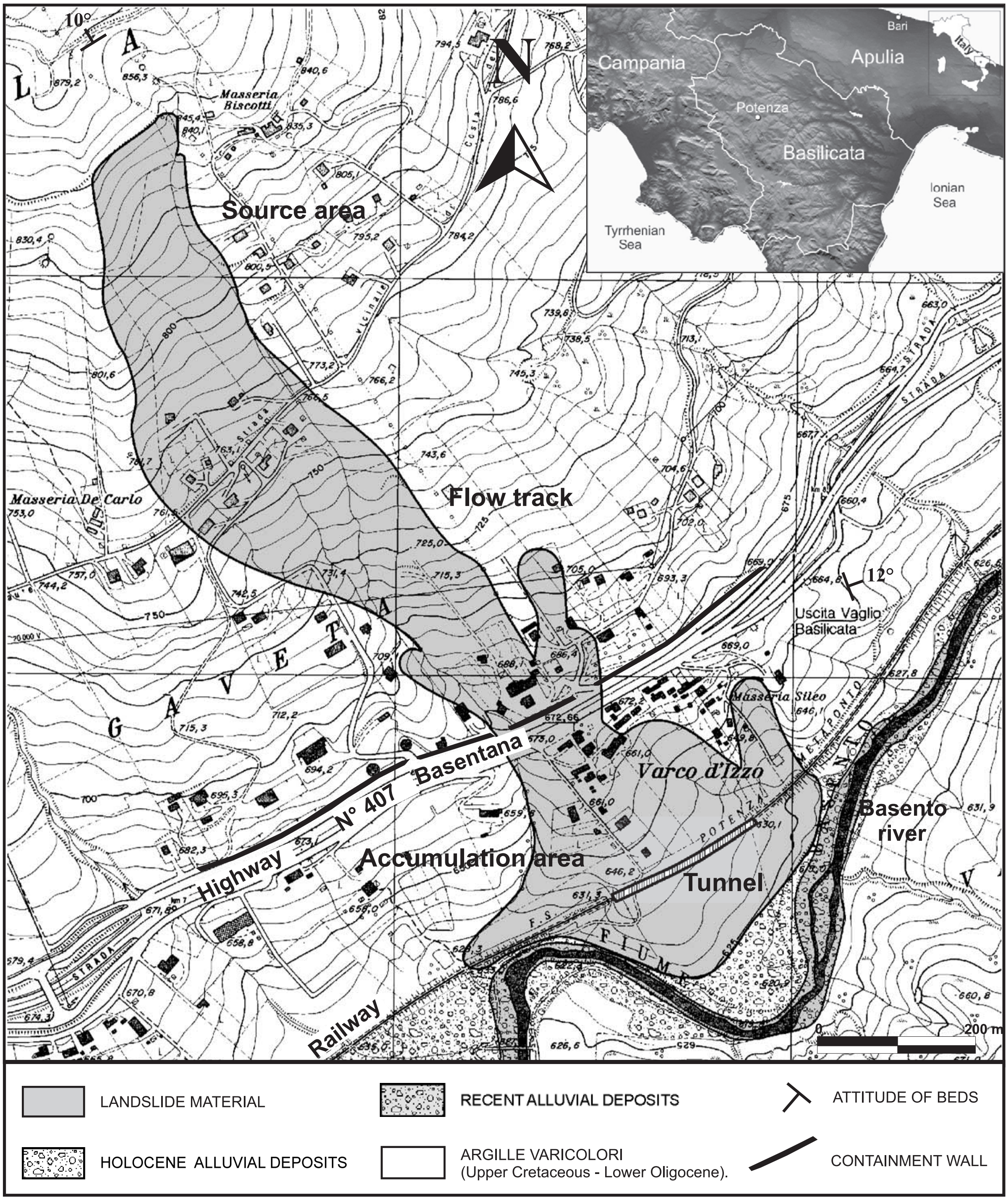

Fig. 1. Location and geological map of the Varco d'Izzo landslide in the Basilicata Region (Southern Apennine, Italy). The landslide develops entirely in the clayey material of the Argille Varicolori formation and, in the accumulation zone, it partly covers recent alluvial deposits.

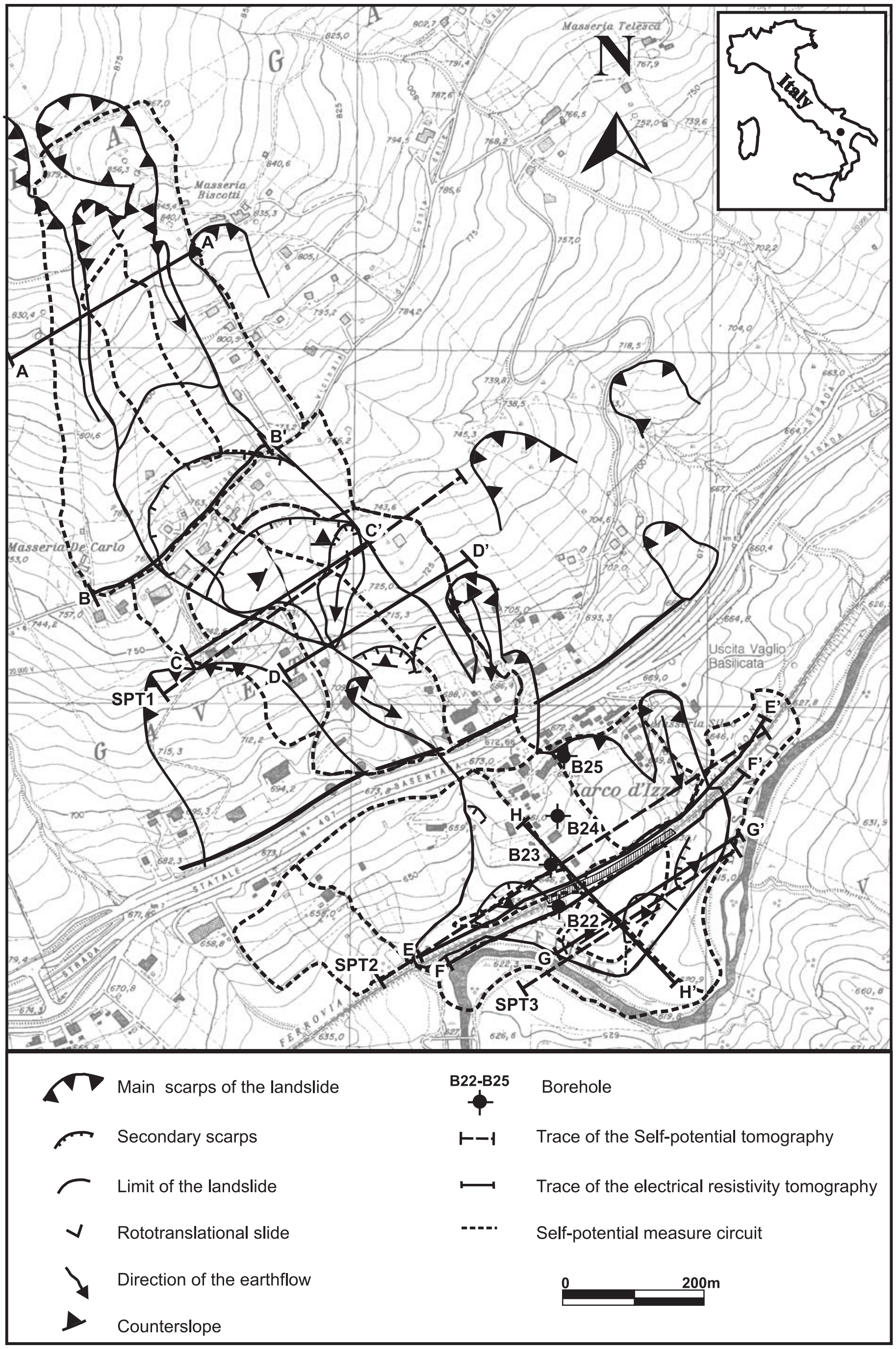

Fig. 2. Geomorphologic map of the Varco d'Izzo landslide with location of the geological and geophysical surveys. SP mapping was carried out on the entire landslide body; seven ERT profiles were performed transversal to the landslide and only one longitudinal; SPT profiles were carried out transversal to the landslide body.

The source area of the mass movement is a rototranslational slide showing an inclination of about 16°. It is approximately 300 m long, about 100–150 m wide and extends from 885 to 820 m a.s.l.

The flow track of the landslide is approximately 700 m long and, on average, its inclination is 12°. In this area, there are some secondary scarps, with different elevations, and a small earthflow extends between 745 and 705 m a.s.l. Many manmade structures, such as the Basentana Road and the buildings along it, have been largely damaged by this movement. The thickness of the sliding material varies from 15 to 25 m.

The zone of accumulation, the widest part of the landslide (about 500 m), is approximately 350 m long and shows an average inclination of 8°. The toe material has diverted the Basento riverbed. The thickness of the displaced material, as shown by the borehole data (B22, B23 and B24 in Fig. 2), varies from approximately 13 m in the upper zone to 32 m in the lower zone. In this section, local reactivations, a few secondary scarps and damage caused to buildings and manmade structures can be observed.

3. Geoelectrical methods

In order to investigate the Varco d'Izzo landslide, three different types of geoelectrical surveys were employed: electrical resistivity tomography (ERT), self-potential mapping (SPM) and self-potential tomography (SPT).

In the next subsections, the mathematical background and the field acquisition procedures will be described and the results from these geoelectrical prospecting techniques will be presented and discussed.

3.1. Electrical resistivity tomography

Electrical resistivity tomography (ERT) is an active prospecting method used for obtaining a high-resolution image of subsurface patterns of electrical resistivity. Recently, this technique has been largely applied for the investigation of areas having complex geology. Interesting results in volcanic and geothermal areas, seismotectonic structures, hydrogeological phenomena and engineering and environmental problems (Di Maio et al., 1998; Caputo et al., 2003; Ogilvy et al., 1999; Steeples, 2001 and references therein) have been obtained.

Under this framework, we applied this method in order to depict the geometric features of the Varco d'Izzo landslide and then to test the resistivity contrast between the shallow mobilized material and the hard-rock substrate. We used a multielectrode system with 32 electrodes and a dipole–dipole array layout with an electrode spacing varying from 10 to 30 m. The choice of the dipole–dipole array was taken based on some balancing factors such as ability to detect both vertical and horizontal resistivity discontinuities (i.e. lateral limits and sliding surface of landslide bodies), depth of investigation, horizontal data coverage, resolution and possibility of performing measures over uneven grounds. For each profile, no less than 323 measurements of apparent resistivities were carried out, following the 2D pseudosection scheme (Sharma, 1997). During data acquisition, great attention was devoted to reducing cultural noise influence. A robust statistical technique was applied in order to extract the useful signal from voltage recordings (Lapenna et al., 1994).

In order to transform the apparent resistivity pseudosection into a model representing the distribution of calculated electrical resistivity in the subsurface, we used RES2Dinv software (Loke and Barker, 1996). The inversion routine is based on the smoothness constrained least-squares inversion (Sasaki, 1992) implemented by using a quasi-Newton optimisation technique. The subsurface is divided into rectangular blocks, the number of which corresponds to the number of measurement points. The optimisation method adjusts the 2D resistivity model trying to iteratively reduce the difference between the calculated and measured apparent resistivity values. The root-mean-squared (RMS) error provides a measurement of this difference.

During the field survey, eight ERTs with lengths varying from 310 to 600 m were carried out; seven ERTs were oriented transversely to the landslide body and only one was oriented parallel to the accumulation zone (Fig. 2).

Fig. 3 shows the inverse model resistivity sections related to the most significant electrical tomographies carried out along profiles AA′, CC′, EE′ and HH′. The BB′ and DD′ tomographies (not shown) do

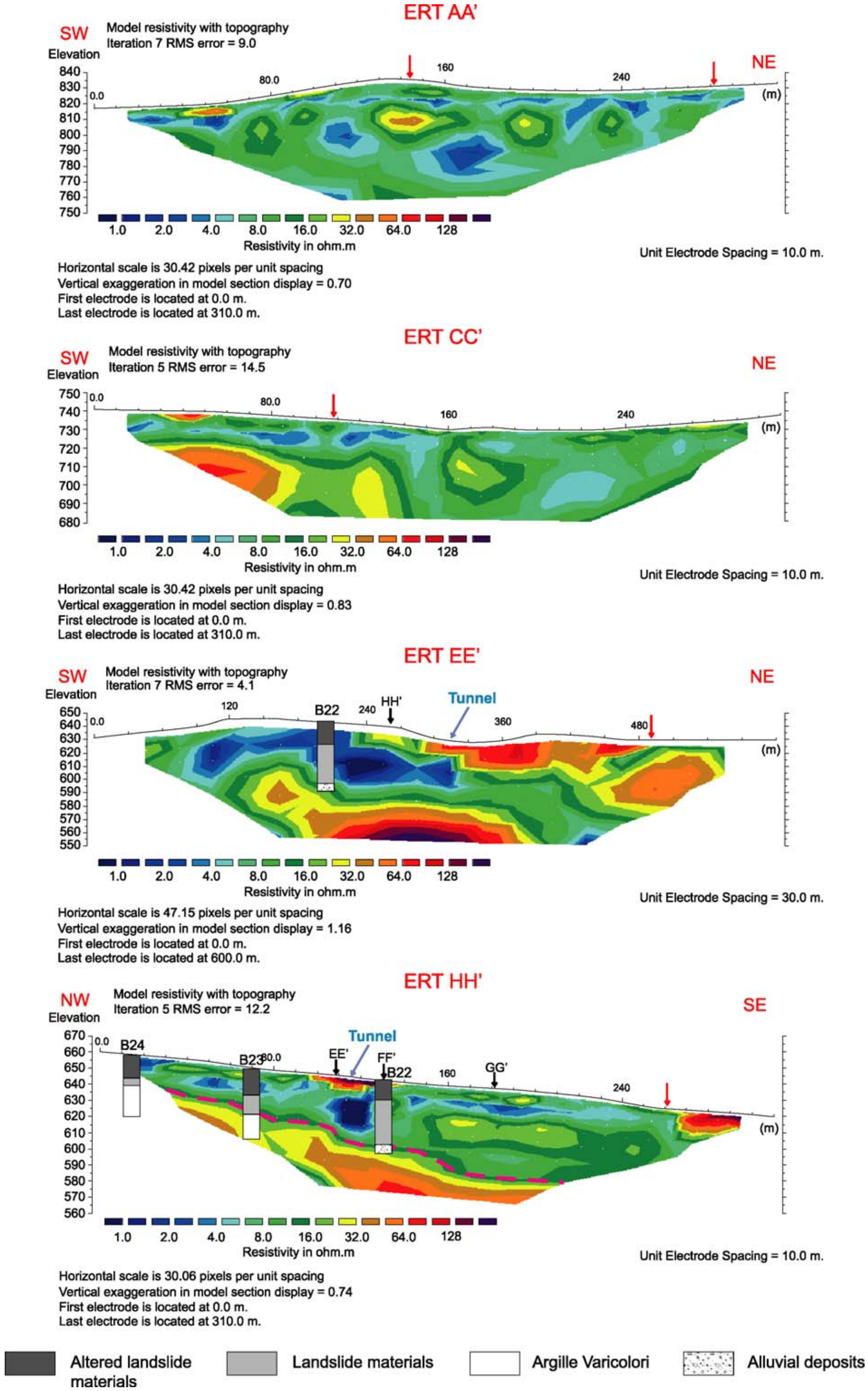
ERT AA'
SW
NE
Model resistivity with topography
Iteration 7 RMS error = 9.0
Elevation
Resistivity in ohm.m
Unit Electrode Spacing = 10.0 m.
Horizontal scale is 30.42 pixels per unit spacing
Vertical exaggeration in model section display = 0.70
First electrode is located at 0.0 m.
Last electrode is located at 310.0 m.
ERT CC'
SW
NE
Model resistivity with topography
Iteration 5 RMS error = 14.5
Elevation
Resistivity in ohm.m
Unit Electrode Spacing = 10.0 m.
Horizontal scale is 30.42 pixels per unit spacing
Vertical exaggeration in model section display = 0.83
First electrode is located at 0.0 m.
Last electrode is located at 310.0 m.
ERT EE'
SW
NE
Model resistivity with topography
Iteration 7 RMS error = 4.1
Elevation
B22
HH'
Tunnel
Resistivity in ohm.m
Unit Electrode Spacing = 30.0 m.
Horizontal scale is 47.15 pixels per unit spacing
Vertical exaggeration in model section display = 1.16
First electrode is located at 0.0 m.
Last electrode is located at 600.0 m.
ERT HH'
NW
SE
Model resistivity with topography
Iteration 5 RMS error = 12.2
Elevation
B24
B23
Tunnel
EE'
FF'
B22
GG'
Resistivity in ohm.m
Unit Electrode Spacing = 10.0 m.
Horizontal scale is 30.06 pixels per unit spacing
Vertical exaggeration in model section display = 0.74
First electrode is located at 0.0 m.
Last electrode is located at 310.0 m.
1.0 2.0 4.0 8.0 16.0 32.0 64.0 128
Altered landslide materials
Landslide materials
Argille Varicolori
Alluvial deposits

not clearly outline the geometry of the landslide; there was a lot of noise interference in the FF′ electrical image (not shown) in the shallow part probably because of the presence of the tunnel, and the GG′ tomography (not shown) was very similar to the EE′. In all cases, the number of iterations varied between 5 and 7 with the RMS error ranging from 14.5% to 4.1%.

A preliminary inspection of the obtained electrical images allows us to identify small variabilities of electrical resistivity for values lower than 150 Ω m. In particular, the very low resistivity values ($\rho<10$ Ω m) observed in the middle part of resistivity tomographies could be associated to the landslide body which is characterized by a high content of clayey material and water. Although there have been no laboratory resistivity measures taken on samples from the investigated area, geochemical and mineralogical analyses show that the Argille Varicolori Formation is characterized by the presence of illite–smectite mixed layers showing a high cationic exchange capacity (CEC) that could notably reduce the resistivity values to a limiting value as low as 0.1 Ω m (Cavalcante et al., 2003; Keller and Frischknecht, 1966). The relatively high resistivity zones ($\rho>60$ Ω m) on the sides and at the bottom of the slide (except in the ERT AA′) may indicate compact rocks not involved in the landslide as has been confirmed by in situ resistivity measurements previously performed for calibration. Some shallow relatively high resistivity nuclei ($\rho>30$ Ω m) may be associated with lapideous intercalations (calcilutitic, calcarenitic blocks, etc.), embedded in the dislocated material. The estimated thickness of the slide deposits, as derived from the resistivity contrasts observed in the ERTs, varies from less than 10 up to 40 m.

The AA′ ERT carried out in the source area of the landslide shows extremely low resistivity material ($\rho<10$ Ω m) and presence of some resistive nuclei (16–32 Ω m). The low resistivity values could be associated to the clayey material, while the resistive nuclei to the presence of calcarenitic blocks. It is not possible to define the lateral limits of the landslide (the red arrow in Fig. 3 shows the geomorphologic boundary) and a possible sliding surface because the terrain in the source area is partially eroded, as was observed by in situ geomorphological surveys.

The CC′ ERT carried out in the flow track of the landslide is characterized by the presence of a shallow layer of low resistivity material ($\rho<10$ Ω m) lying above an irregular resistive material (16–128 Ω m). This can be explained by the presence of clayey material lying over calcareous material. In the central part of the tomography, a remarkable vertical resistivity contrast is present. This phenomenon is possibly related to the presence of an underlying vertical contact (fault) having high water content. Also in this case, the presence of some shallow resistive nuclei (16–32 Ω m) may be associated with calcareous material.

The transverse EE′ ERT, carried out in the accumulation zone of the landslide, outlines a resistivity contrast in the SW side between a shallow relatively low resistivity layer ($\rho<16$ Ω m) and a deeper relatively high resistivity zone ($\rho>30$ Ω m). The limits of these zones are not well defined, but the resistivity slowly increases at a depth of about 30 m. The low resistivity zone has a lenticular shape and it could be associated to the landslide body because it has a high level of clay content and a high degree of saturation, while the high resistivity zone could be related to the alluvial material not involved in the movement. This result is confirmed by the geological data obtained from borehole B22 that reports a sliding surface at a depth of about 32 m, with 11 m of altered landslide material overlying 21 m of landslide material. In the deeper part of the borehole, there is 4 m of alluvial terrain. Then, the sliding surface coincides with the transition zone where we observe an increase in resistivity. The central part of the ERT shows a shallow relatively high resistivity zone (16–64 Ω m) having a maximum height of about 12 m and a width of about 200 m which is probably associated

Fig. 3. Dipole–dipole ERTs carried out perpendicular (AA′, CC′and EE′) and parallel (HH′) to the direction of the landslide body. We adopted the same colour palette for all the electrical sections. The red arrows indicate the lateral limits of the landslide as derived from geomorphological observations. The data coming from boreholes B22, B23 and B24 are also included. The dashed red line represents the interpreted sliding surface in the accumulation zone of the landslide body. For profile location, see Fig. 2.

with the presence of the railway tunnel. The high resistive values ($\rho > 30\ \Omega$ m) in the NE shallow side of the tomography could be explained by the presence of calcareous material outcropping in this area.

The HH′ ERT is the only longitudinal ERT performed on the landslide. It shows a conductive layer ($\rho < 16\ \Omega$ m) having a thickness varying from about 20 m on the top to 50 m towards the toe of the landslide which overlies a relatively high resistive layer ($\rho > 16\ \Omega$ m). The conductive zone has an irregular shape and could correspond to the mobilized body, while the deep resistive zone could be related to compact deposits (alluvial and clayey material) which are not involved in the landslide. This agrees strongly with the stratigraphic data obtained from boreholes B22, B23 and B24. In particular, borehole B23 reports the sliding surface at a depth of about 30 m with about 17 m of altered landslide material which overlies about 13 m of landslide material, and about 11 m of the clayey material that may correspond to the Argille Varicolori Formation are seen in the deeper part. In borehole B24, the sliding surface is reported to be at a depth of about 21 m. It shows 16 m of altered landslide material which overlies 5 m of landslide material, and in the deeper part, about 21 m of Argille Varicolori can be seen. Moreover, the SE toe limit of the landslide is well defined and shows a high resistivity contrast between the clayey body earthflow and the alluvial materials of the Basento River. Finally, the shallow resistive nucleus ($\rho > 64\ \Omega$ m), located about 110–120 m from the origin of the profile, is related to the railway tunnel running across the landslide.

3.2. Self-potential survey

The self-potential (SP) method consists in measuring natural electrical fields developed in the subsurface by several mechanisms: electrokinetic coupling (streaming potential), thermoelectric coupling, electrochemical effects, cultural activity, etc. (Corwin and Hoover, 1979). In past years, the SP method has been applied in a wide class of geological problems: mineral prospecting, detection and delineation of thermal sources in geothermal and volcanic areas and hydrogeological studies for groundwater investigations (Zlotnicki et al., 1994; Loddo et al., 1996; Di Maio et al., 1996; Revil et al., 2002). In landslide areas, spatial and temporal measurements of the SP field may provide information on dynamic aspects of the hydrogeologic conditions within the landslide body (Bogoslovsky and Ogilvy, 1977; Coppola et al., 1994; Patella et al., 1995; Sharma, 1997; Gallipoli et al., 2000).

In these latter investigations, the SP anomalies are mainly due to the streaming potentials generated by fluid flows in porous rocks, as a consequence of pore pressure gradient. This electrokinetic effect is controlled by the relative motion occurring along a shear plane between the charged mineral surface (negative in silica mineral, such as clays) and associated with an electrical diffuse layer in the pore fluid (positive in clays). The ζ potential is the electrical potential on the shear plane (Revil et al., 1999) and is related to the streaming potential V as follows:

$$V = \frac{\rho \varepsilon \zeta}{\eta} \Delta P$$

where ρ, ε and η are the electrical resistivity, dielectric permittivity and dynamic viscosity of the pore fluid, respectively, and ΔP is the drop in pressure along the flow path.

In this scheme, positive charges are carried in the direction of the fluid flow, producing positive SP anomalies on the surface where water discharge is located and negative in the sites of infiltration (Loddo et al., 1996; Sharma, 1997; Revil and Leroy, 2001).

Recently, some authors have proposed new algorithms for SP data inversion (Patella, 1997) and new geophysical models in order to describe the generating mechanism of SP anomalous patterns (Revil et al., 2002). These recent developments lead to more quantitative interpretations of hydrogeological applications, with the study of the main features of fluid flow in landslide bodies included.

In this paper, two different measuring strategies were adopted during the field surveys: SP mapping (SPM) and SP tomography (SPT). The first one is mainly used for delineating the boundaries of the landslide and the local groundwater system. The second one is a powerful tool for identifying the location and form of any electrical accumulation zones in the investigated area.

The field acquisition procedure for the SPM technique is described below. Potential horizontal gradients were measured along both closed loops and linked traverses by alternating the leading and following electrodes (leap-frog technique) in order to reduce cumulative errors caused by electrode polarization. The distance between the measuring electrodes was 50 m. The SP values in the measuring net were obtained by adding readings after establishing a SP arbitrary zero value as a point of reference in the area. Moreover, SP measurements were corrected in order to compensate for cumulative errors. This is done by distributing the closure errors linearly along each circuit. In order to obtain a better visualization of the SP anomalies, we subtracted the net average value of the whole set of SP data from the potential obtained in each point. Finally, using a contour line representation of the distribution of the potential field, we obtained a SP map.

For the application of the SPT technique, we adopted the previous measurement strategy moving the measuring dipole along selected profiles with length varying in range from 400 to 600 m, using an electrode spacing of 20 m in order to increase the resolution of the tomographic approach.

In a second step, the SP profiles were inverted using the 2D probability tomography technique proposed by Patella (1997). The mathematical background of this technique is based on the decomposition of the SP field into a sum of elementary contributions which are derived from a discretised distribution of charge accumulation centres. The inversion problem consists in recovering the most probable discretised charge distribution underground which is responsible for the measured SP field. The 2D tomography is based on a cross-correlation algorithm between a theoretical scanner function and the observed electric field along the profile. The cross-correlation integral gives an estimate of the charge occurrence probability (COP) function which represents the probability of finding a positive (COP values > 0) or negative (COP values < 0) electric charge accumulation in each point of a cross section along the profile.

On the Varco d'Izzo landslide, a SPM and three SPTs (Fig. 2), transversely oriented to the landslide body, have been carried out.

The SPM (Fig. 4) shows a spatial pattern characterized by slightly negative SP values in the source area, a positive zone in the flow track area and a strong SP negative zone in the accumulation area of the slide. The SP negative values in the source area are probably due to water infiltration in the detachment zone (Sharma, 1997). The SP positive zone in the flow track may be due to the containment walls and drainage structures, built for the SS 407 Basentana road, that prevent groundwater from flowing into the accumulation area, which in turn produces an accumulation and excess of positive electrical charges.

On the other hand, the SP negative sector in the accumulation zone, which seems to follow the slide outline perfectly, may be explained by a groundwater flow towards the Basento River having an excess of positive electric charges.

Fig. 5 is the 2D representation of the COP values for the three SPT profiles. In each panel, the horizontal axis is the survey line and the vertical axis is the depth from ground level. For the computation, we used a square grid with the side measuring 20 m, equal to the field sampling interval.

Qualitatively, the panels, which reach a maximum investigation depth of about 120 m bgl, show an irregularly spaced alternating sequence of shallow positive and negative SP source centres, some of which could be associated with the presence of calcareous mudstone, calcarenitic blocks embedded in the altered material, as already indicated by the ERTs. Moreover, in the central part of the SPT1, across the flow track, a dipolar field can be observed, which reflects the presence of a probable vertical structure that is also detected by the ERT CC′. The presence of a prevalently negative charge concentration within the landslide body can be observed in the SPT2 and SPT3 carried out on the toe of the landslide. The centre of these nuclei, reaching a depth not exceeding 30–40 m, may be related to the slip surface, as observed in borehole data and ERT results. The tomography results in Fig. 5 also show that the lateral boundaries of the landslide appear to be in the same position of strong horizontal changes in the COP function. Based on this preliminary analysis, the spatial charge distribution in the subsoil along the SPT profiles seems to be directly related to geological discontinuities.

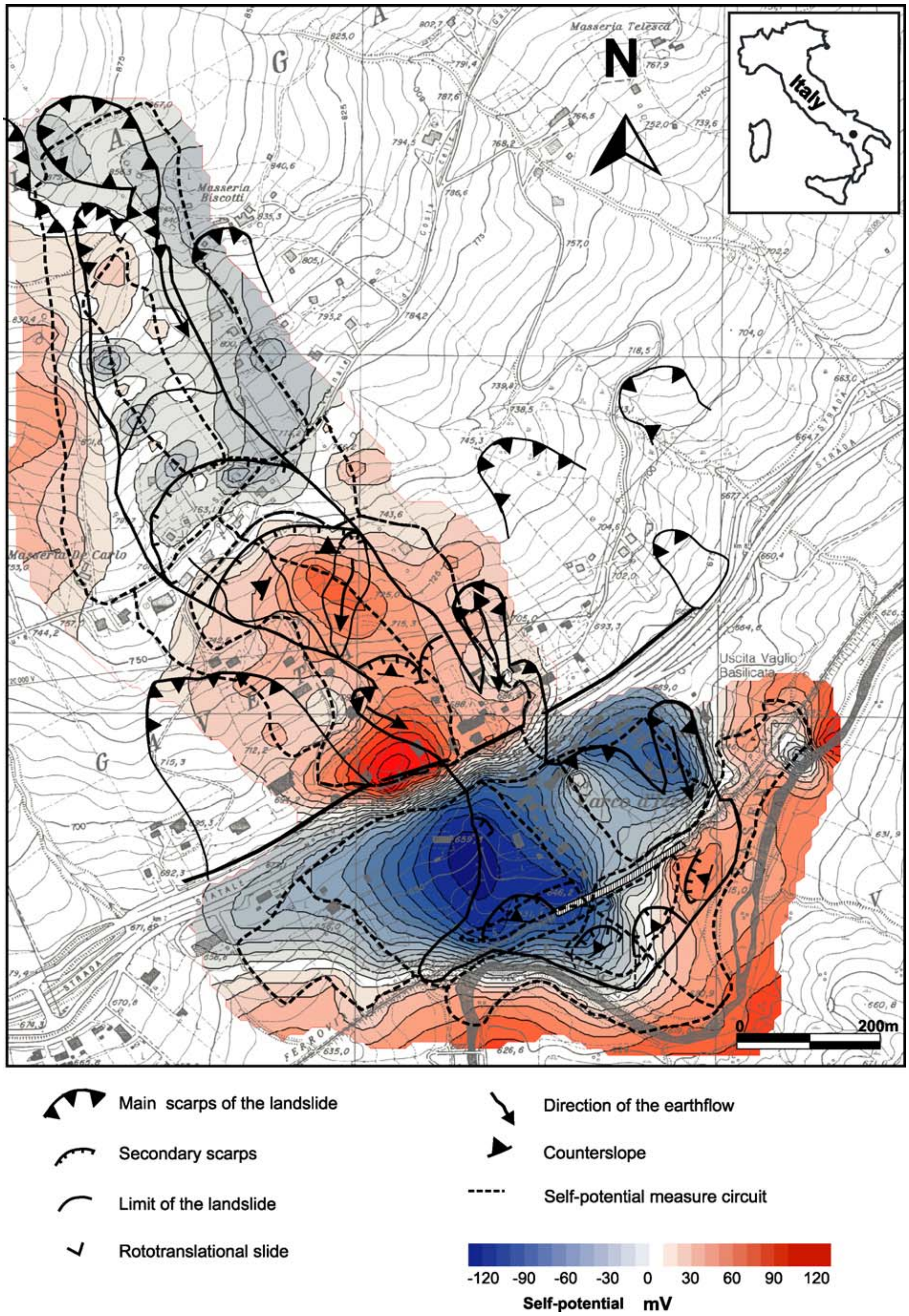

Fig. 4. Map of the SP anomalies relative to the areal survey. Red zones are positive values, whereas blue zones are negative values.

This is clearly only a very qualitative description of the SP anomaly field. We lack of detailed information on the local hydrogeological setting and hydraulic parameters. Moreover, we do not yet have direct measurements of the ζ potential, which is a key parameter of electrokinetic phenomena (Revil et al.,

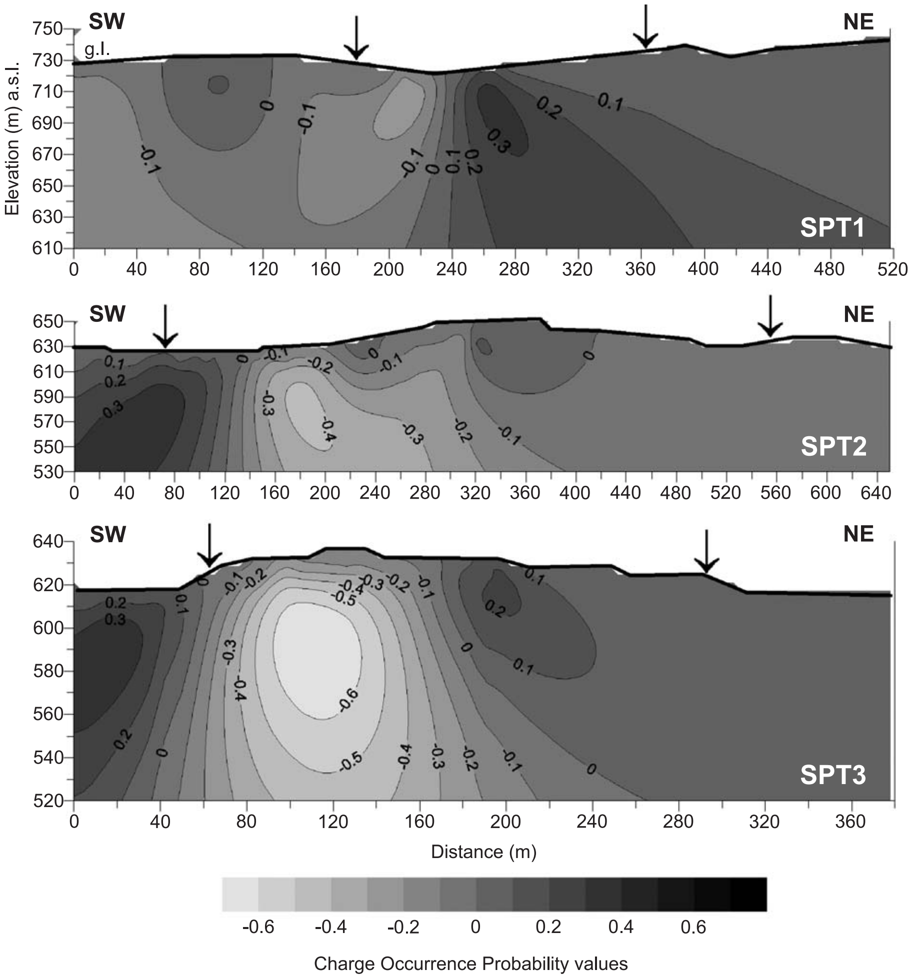

Fig. 5. SPTs carried out transversal to the toe of the landslide. The black arrows represent the lateral limits of the landslide. For profile location, see Fig. 2.

1999), as well as a significant theoretical basis for the evaluation of the correlation between charge accumulations and local hydrogeological settings.

4. Conclusions

We have combined three different geoelectrical prospecting methods with the aim of reconstructing the geometry of the landslide body and describing the main patterns of the subsurface fluid flows in the landslide area.

The high resolution of the electrical images and the integration of geophysical data with geological, geomorphological and borehole data allowed us to define well the shape of the slide surface and the limits of the landslides especially in the accumulation zone. Electrical resistivity tomography does not allow to define the shape of the source area, where the superficial erosion has erased the form of the landslide. The SPM and SPT techniques helped to better understand the groundwater circulation system, although the complexity of the problem does require more hydrogeological measurements. In particular, the SPM allowed us to locate the zones having high water content, which is linked to an excess in positive electrical charges. The SPT allowed us to define well the lateral limits of the landslide body which correspond to the position of strong horizontal changes in the COP function.

To close, we emphasize that an integrated approach based on non-invasive electrical prospecting methods, geological investigations and geomorphologic information seems to be a promising tool for investigating landslide areas with complex geology. In the future, using a monitoring strategy designed to continuously repeat electrical surveillance, it will be possible to study temporal fluctuations of the subsurface resistivity values. Time-lapse analysis of 2D and 3D electrical images, carried out across landslide bodies, could enable to better understand the time dynamics of the hydrogeological processes which are behind the causes of instability phenomena.

Acknowledgements

This work was supported by the project "Design of a geophysical monitoring network in areas with high hydrogeological risk in the Basilicata region" funded by Italian Ministry of Instruction, University and Research (MIUR).

References

Bogoslovsky, V.A., Ogilvy, A.-A., 1977. Geophysical methods in the investigation of landslides. Geophysics 42, 562–571.

Bonardi, G., D'Argenio, B., Perrone, V., 1988. Carta geologica dell'Appennino meridionale alla scala 1:250.000. Memorie della Società Geologica Italiana 41, 1341.

Bruno, F., Marillier, F., 2000. Test of high-resolution seismic reflection and other geophysical techniques on the Boup landslide in the Swiss Alps. Surveys in Geophysics 21, 333–348.

Bruno, F., Levato, L., Marillier, F., 1998. High resolution seismic reflection, EM and electrokinetic SP applied to landslide studies: "Le Boup" landslide (Western Swiss Alps). In: Casas, A. (Ed.), Proceedings of the IV Environmental and Engineering Geophysical Society (European Section), September 14–17, Barcelona (Spain), pp. 571–574.

Caputo, R., Piscitelli, S., Oliveto, A., Rizzo, E., Lapenna, V., 2003. High-resolution resistivity tomographies in active tectonic studies. Examples from the Tyrnavos Basin, Greece. Journal of Geodynamics 36, 19–35.

Cavalcante, F., Fiore, S., Piccarreta, G., Tateo, F., 2003. Geochemical and mineralogical approaches to assessing provenance and deposition of shales: a case study. Clay Minerals 38, 383–397.

Coppola, B., Lapenna, V., Mancini, M., Patella, D., 1994. Application of unconventional geoelectrical methods to the hydrogeological examination of the Mt. S. Crocerock formations (Umbria, Italy) involved in a railway tunnel project. Annali di Geofisica 37 (5), 1251–1267.

Corwin, R.F., Hoover, D.B., 1979. The self-potential method in geothermal exploration. Geophysics 44, 226–245.

Cruden, D.M., Varnes, D.J., 1996. Landslide types and processes. Landslide: Investigation and Mitigation. In: Turner, A.K., Schuster, R.L. (Eds.), National Research Council, Transportation Research Board, Special Report 247, 36–75.

Curcetti, C., 1996. Franosità pregressa ed attuale dell'alta valle del fiume Basento: La frana di Varco d'Izzo. Unpublished Degree Thesis. Faculty of Engineering of the Basilicata University, Potenza (Italy).

Di Maio, R., Di Sevo, V., Giammetti, S., Patella, D., Piscitelli, S., Silenziario, C., 1996. Self-potential anomalies in some Italian volcanic areas. Proc. of the 5th National Meeting of Geoelectromagnetism (Martina Franca, September 1993). Annali di Geofisica 39 (1), 179–188.

Di Maio, R., Mauriello, P., Patella, D., Petrillo, Z., Piscitelli, S., Siniscalchi, A., 1998. Electric and electromagnetic outline of the Mount Somma-Vesuvius structural setting. Journal of Volcanology and Geothermal Research 82 (1–4), 219–238.

Gallipoli, M., Lapenna, V., Lorenzo, P., Mucciarelli, M., Perrone, A., Piscitelli, S., Sdao, F., 2000. Comparison of geological and geophysical prospecting techniques in the study of a landslide in southern Italy. European Journal of Environmental and Engineering Geophysics 4, 117–128.

Giano, S.I., Lapenna, V., Piscitelli, S., Schiattarella, M., 2000. Electrical imaging and self-potential surveys to study the geological setting of the Quaternary slope deposits in the Agri high valley (Southern Italy). Annali di Geofisica 43, 409–419.

Griffiths, D.H., Barker, R.D., 1993. Two-dimensional resistivity imaging and modelling in areas of complex geology. Journal of Applied Geophysics 29, 211–226.

Gullà, G., and Sdao, F., 2001. 'Dissesti prodotti o aggravati dal sisma del 9 Settembre 1998 nel territorio del confine Calabro-Lucano: Monografia del Gruppo Nazionale Difesa Catastrofi Idrogeologiche', Cnr- U.O. 2.56. Pubbl. N. 2121 del Catalogo Pubblicazioni del GNDCI, Cnr. 113 pp.

Hack, R., 2000. Geophysics for slope stability. Surveys in Geophysics 21, 423–448.

Keller, G.V., Frischknecht, F.C., 1966. Electrical Methods in Geophysical Prospecting. Pergamon Press, Oxford, p. 517.

Lapenna, V., Macchiato, M., Patella, D., Satriano, C., Serio, C., Tramutoli, V., 1994. Statistical analysis of non-stationary voltage recordings in geoelectrical prospecting. Geophysical Prospecting 42 (8), 917–952.

Lapenna, V., Lorenzo, P., Perrone, A., Piscitelli, S., Sdao, F., Rizzo, E., 2003. High-resolution geoelectrical tomographies in the study of the Giarrossa landslide (Potenza, Basilicata). Online version of Bulletin of Engineering Geology and the Environments. Official Journal of IAEG, Springer Verlag. Berlino-Germania. DOI 10.1007/s10064-002-0184-z.

Loddo, M., Quarto, R., Schiavone, D., 1996. Integrated geophysical survey for the geological structural and hydrogeothermal study of the north-western Gargano promontory (Southern Italy). Annali di Geofisica 39 (1), 201–219.

Loke, M.H., Barker, R.D., 1996. Rapid least-squares inversion of apparent resistivity pseudosections by a quasi-Newton method. Geophysical Prospecting 44 (1), 131–152.

Mauritsch, H.J., Seiberl, W., Arndt, R., Romer, A., Schneiderbauer, K., Sendlhofer, G.P., 2000. Geophysical investigations of large landslides in the Carnic Region of southern Austria. Engineering Geology 56, 373–388.

McCann, D.M., Forster, A., 1990. Reconnaissance geophysical methods in landslide investigations. Engineering Geology 29 (1), 59–78.

Ogilvy, R., Meldrum, P., Chambers, J., 1999. Imaging of industrial waste deposits and buried quarry geometry by 3-D resistivity tomography. European Journal of Environmental and Engineering Geophysics 3, 103–113.

Patella, D., 1997. Introduction to ground surface self-potential tomography. Geophysical Prospecting 45, 653–681.

Patella, D., Di Maio, R., Alfinito, A., 1995. Misure di potenziale spontaneo su un versante in frana. In: Bonardi, G., De Vivo, B., Gasparini e A. Vallario, P. (Eds.), Cinquanta Anni di Attività Didattica e Scientifica del Prof. Felice Ippolito. Liguori, Naples, pp. 183–196.

Polemio, M., Sdao, F., 1996. Landslide hazard and critical rainfall in Southern Italy. VII Int. Symp. on Landslides, Norway. Balkema, Rotterdam, pp. 847–852.

Revil, A., Leroy, P., 2001. Hydroelectric coupling in a clayey material. Geophysical Research Letters 28 (8), 1643–1646.

Revil, A., Pezard, P.A., Glower, P.W.J., 1999. Streaming potential in porous media: 1. Theory of the zeta potential. Journal of Geophysical Research 104, 20021–20031.

Revil, A., Hermitte, D., Voltz, M., Moussa, R., Lacas, J.G., Bourrié, G., Trolard, F., 2002. Self-potential signals associated with variations of the hydraulic head during an infiltration experiment. Geophysical Research Letters 29 (7), 1106.

Sasaki, Y., 1992. Resolution of resistivity tomography inferred from numerical simulation. Geophysical Prospecting 54, 453–464.

Schmutz, M., Albouy, Y., Guerin, R., Maquaire, O., Vassal, J., Schott, J.J., Descloitres, M., 2000. Joint electrical and time domain electromagnetism (TDEM) data inversion applied to the Super Sauze earthflow (France). Surveys in Geophysics 21, 371–390.

Sharma, P.S., 1997. Environmental and Engineering Geophysics. Cambridge Univ. Press, p. 475.

Steeples, D.W., 2001. Engineering and environmental geophysics at the millennium. Geophysics 66 (1), 31–35.

Zlotnicki, J., Feuillard, M., Hammouya, G., 1994. Water circulations on La Soufrière volcano inferred by self-potential surveys (Guadeloupe, Lesser Antilles). Renew of volcanic activity? Journal of Geomagnetism and Geoelectricity 46, 797–813.